ACOUSTIC CHARACTERIZATION OF AN ARTIFICIAL CO_2 SEEP USING SPLIT-BEAM ECHO SOUNDERS

Scott Loranger[a], Ann Elisabeth Albright Blomberg[b], Geir Pedersen[c], Ivar-Kristian Waarum[b] and Andreas Austeng[d]

[a] University of New Hampshire, 24 Colovos Road, Durham NH 03824.
[b] Norwegian Geotechnical Institute, Sognsveien 72, 0855 Oslo, Norway
[c] NORCE Norwegian Research Centre, P.O. Box 6031, Bergen 5892, Norway
[d]University of Oslo, POBox 1080 Blindern, NO-0316 Oslo, Norway

Scott Loranger, University of New Hampshire, 24 Colovos Road, Durham NH 03824. Ph: 1-603-862-3353. Email: sloranger@ccom.unh.edu

Abstract: *Geological carbon storage (GCS) has emerged as a promising method for reducing greenhouse gas emissions and achieving international climate goals. Currently, sub-seafloor GCS sites sequester about 1.8 MtCO_2/yr. Additional sites are under development and by 2050, there is potential for storage of ≈ 100 Mt CO_2/yr. For the expansion of sub-seafloor GCS to be successful, cost-efficient and effective leak monitoring systems must be available. The ACT4storage project is tasked with development of leak monitoring through the selection and use of available technologies. A part of the monitoring suite is the use of active acoustics to detect and quantify free CO_2 bubbles and droplets. An artificial seep device was created to simulate leaks of CO_2 bubbles. Leak simulations were quantified by two broadband split-beam echosounders (50-90 kHz and 250-450 kHz). The split-beam echosounders offer high sensitivity, broadband transmission and were calibrated to quantify flux from a leakage site. The split-beam echosounders show promise as cost-efficient and effective methods for the detection and quantification of free CO_2.*

Keywords: *Geological carbon storage, broadband, echo sounder, leak detection*

INTRODUCTION

Geological carbon storage (GCS) has emerged as a promising method for reducing greenhouse gas emissions[1]. GCS involves capturing CO_2 from industrial point sources (such as power plants) and injecting the CO_2 into geological storage sites. Potential sites include saline aquafers, coal seams, and oil and gas reservoirs. The overall goal of GCS is to return the CO_2 to long-term geological storage and to minimize the net flux of CO_2 to the atmosphere. Currently, there are three major GCS sites – the Sleipner and Snøhvit fields off the coast of Norway in the North Sea and Norwegian Sea respectively, as well as the pilot K12-B project offshore of the Netherlands [2]. The Sleipner field is the largest, accounting for ~ 1Mt/yr of CO_2 storage since 1996. As carbon capture and storage technology advances, there is the potential for much greater storage, including up to ~240 Gt of CO_2 in Europe alone [3], [4].

In order to assess the effectiveness of GCS, sequestration sites must be monitored for leaks of CO2. Current European Union regulations require that monitoring strategies cover the injection site, geological reservoir and surroundings[5]. Current monitoring practice includes a variety of technologies such as downhole monitoring, seismic surveying and environmental monitoring of the seabed and water column[6]–[8]. The ACT4storage (Acoustic and Chemical Technologies for environmental monitoring of geological carbon storage) project is tasked with evaluating available technologies GCS environmental monitoring of the seabed and water column to determine the most reliable, effective and cost efficient monitoring methods. As part of the ACT4Storage program, the use of acoustic instrumentation for the detection and quantification of CO_2 is currently being assessed. An artificial leak of CO_2 was generated in about 20 m water depth and broadband acoustic sensors used to detect and quantify the artificial seep.

The depth of the storage site is of especial importance in determining the appropriate frequency for leak monitoring. Below about 600 m CO_2 is in liquid form, and a higher frequency instrument would likely be needed in order to detect a leak. At small *ka*, where *k* is the acoustic wave number and *a* is the droplet radius, liquid droplets have a relatively low target strength (TS) [9], [10]. Target strength is the ratio of scattered intensity to incident intensity and is measure of the efficiency with which a target scatters sound. At higher *ka*, droplets are more efficient scatterers. To detect a leak at depths below 600 m, higher frequencies are likely necessary. This experiment used a high (333 kHz center frequency) and low (70 kHz center frequency) frequency echo sounder to evaluate the instruments likely to be used in either a gas or liquid CO_2 release scenario.

EXPERIMENTAL SETUP

Experiments were conducted at Horten inner harbor near Horten, Norway on October 15 and 19, 2018. The inner harbor is a sheltered environment with limited ocean currents, and low ambient noise levels. The experiment consisted of four seafloor-mounted frames; two chemical sensor frames, a CO_2 plume-generating frame and an acoustic sensor frame. The frames were deployed at depths between 16 m and 20 m. The acoustic sensor frame was 70 m (horizontally)

from the leak frame, with acoustic sensors oriented such that the beam at 70 m was just above the leak frame and below the water surface (Fig. 1).

Two split-beam echo sounders (SBES; Kongsberg Maritime ES70-7C and ES333-7CD – where 70 and 333 indicate the center frequency of the echo sounder) were mounted on the acoustic sensor frame. The SBESs were connected to Kongsberg wide band transceivers (EK80 WBT) to enable frequency modulated broadband (FM) transmission and reception. The echo sounders were calibrated according to the method described by Demer et al 2015 [11]. The SBESs transmitted simultaneous one-millisecond FM pulses from 45 kHz to 95 kHz and 280 kHz to 450 kHz. The ES70 was also run in narrowband (CW) mode to generate a one-millisecond narrow band pulse at the center frequency to compare the signal to noise ratio for FM and CW pulses.

The SBES have a two-way beamwidth of five degrees, resulting in a six m diameter beam at 70 m. The beam was oriented so that the deepest part of the beam was just above the top of the leak frame, and the 6 m beam covered depths from 15 to 9 m, in order to prevent interference from the sea surface and/or the leak frame.

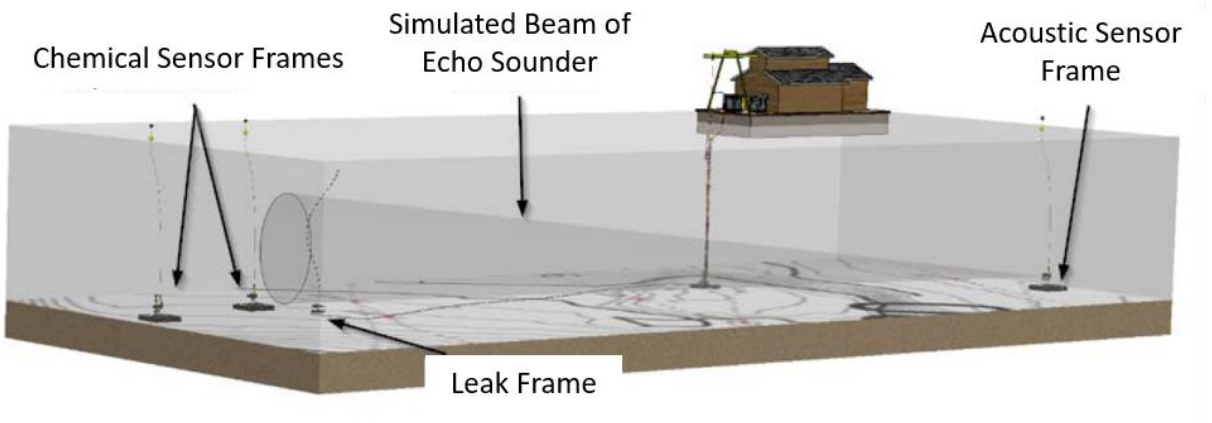

Fig. 1: Orientation of instrument frames. The horizontal distance from the acoustic sensor frame to the leak frame was 70 m.

The simulated CO_2 leak was generated by releasing CO_2 from pressurized bottles mounted on a surface barge anchored in the experiment site. The surface barge pumped CO_2 to the seafloor-mounted leak frame and released the CO_2 from a 3-mm orifice on the frame. A surface pressure regulator controlled the backing pressure applied by the CO_2 bottles to the leak generating system. A camera mounted on the leak frame monitored the orifice for the release of bubbles, and the backing pressure gradually increased until flow from the orifice began. For flows from 0.115 l/min to 1.15 l/min the minimum pressure (1.7 bars) required to generate flow out of the orifice in the leak frame was applied to the system. The pressure required to generate flow was assumed to be slightly greater than the hydrostatic pressure, indicating that the orifice was at a depth of slightly shallower than 17 m.

FLOW RATE

The flow meter had a maximum measureable flow rate of 1.15 l/min. Higher flows were generated by fully opening the flow meter so that it did not restrict flow. The pressure was then increased above 1.7 bars. The flow rate at higher pressures was determined by assuming that pressure was constant from the pressure regulator to the leak frame orifice, and therefore the density of CO_2 was constant. The Bernoulli equation was then used to determine that a change in pressure, ΔP, was proportional to the square root of a change in velocity, $\Delta \mathbf{U}$;

$$\Delta P \propto \sqrt{\Delta \boldsymbol{U}}. \quad (1)$$

For flows from 0.115 to 1.15 l/min, the pressure applied to the system for these flow rates was just high enough for gas to be expelled into the water column and the buoyant force was the dominant force driving the release of bubbles. For higher flows (1.15 l/min to 2.64 l/min), greater pressure was applied by the pressure regulator and that backing pressure was the dominant driving force. The result was two difference force balances at the orifice; the first was the buoyancy dominated forcing where droplets were released with an initial velocity near zero and the second regime is the backing pressure dominated forcing where droplets were expelled with an initial velocity greater than that of the buoyancy dominated forcing.

NOISE LEVEL

Both EK80s were able to detect the gas seep at 70 meters, regardless of flow rate.

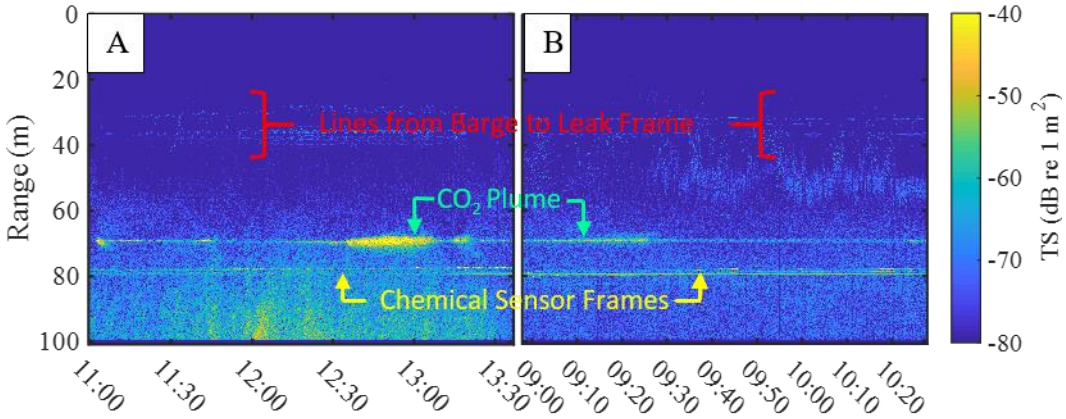

Fig. 2: Echograms from Oct 15, 2018 (A) and Oct 19, 2018 (B) for the ES70. The seep can be seen at 70 meters with intensity changes as the flow rate changes. The chemical sensor frames can be seen at around 80 meters, and returns from mooring ropes and the line connecting the leak frame to the barge are seen between 20 and 40 meters.

The noise level for each echo sounder was computed from the echograms in Fig 2 for ranges where no targets were in the acoustic beam (45 to 65 m). The average (computed in linear space) noise with no time variable gain (TVG) of all samples between 55 and 65 m was calculated for each ping, and then 100 pings were averaged together for both days the experiments to determine the distribution of noise level estimates (Fig 3). The median noise level for both days combined was -151 dB for the ES70 and -149 dB for the ES333.

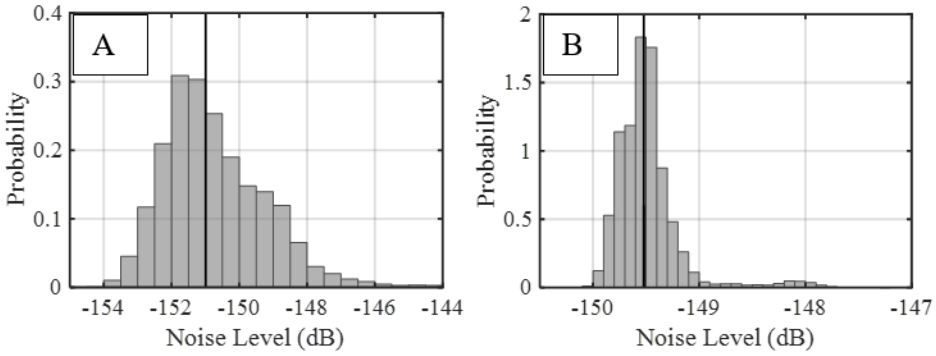

Fig 3. Sound pressure level measurements averaged from samples taken between 55 and 65 meters depth and averaged over 100 pings for the ES70 (A) and the ES 333 (B). The black line shows the median value for the distribution (-151 dB for the 70 kHz echosounder and -149 dB for the 333 kHz).

FLOW RATE AND TARGET STRENGTH

In order to determine the relationship between backscatter and flow rate, the TS of the plume was evaluated. TS is determined by the backscattering cross-sectional area, $\boldsymbol{\sigma_{bs,i}}$, of each target, $\boldsymbol{i}$, in the acoustic sample according to,

$$TS = 10\ log_{10}\left[\sum_{i=1}^{N} \sigma_{bs,i}\right], \quad (2)$$

where N is the total number of scatterers in the acoustic sample. If $\boldsymbol{\sigma_{bs,i}}$ is normally distributed then TS can be approximated from the average backscattering cross-sectional area $\bar{\sigma}$,

$$TS = 10\ log_{10}[N\ \bar{\sigma}]. \quad (3)$$

The target strength of the CO_2 plume generated by the leak frame as a function of flow rate was calculated by applying TVG (accounting for spherical spreading and absorption) and averaging (in linear space) the TS for all pings recorded during the time interval of a given flow rate (Fig. 4).

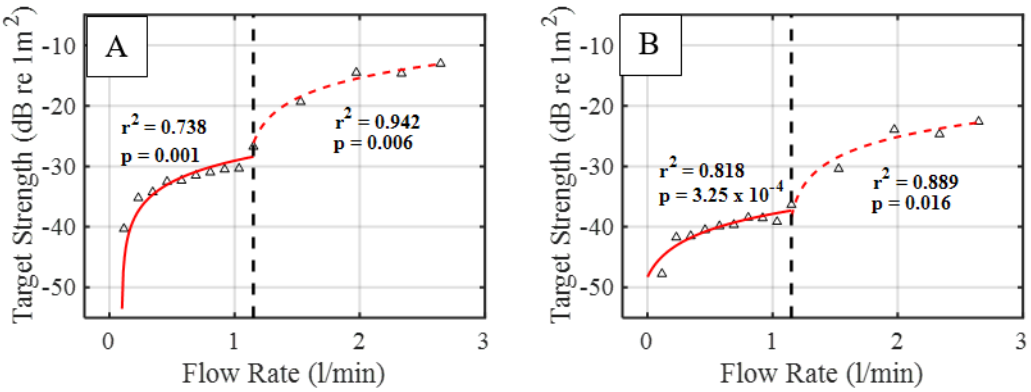

Fig 4: Average target strength as a function of the flow rate (black triangles) for the ES70 (A) and ES333 (B). The backscattering cross sectional area (linear component of TS) was linearly fit to flow rate for the two different forcing regimes: flow driven by the buoyance of the gas (solid red line) and flow driven by backing pressure (dashed red line).The dashed black line shows the division between the two forcing regimes.

The linear component of TS, ($N\overline{\sigma}$ in Eq. (3)) was fit to a line for the two different forcing regimes (buoyancy driven and backing pressure driven described above). The high correlation between TS and flow rate for the two forcing regimes indicates that $N\overline{\sigma}$ and flow rate are linearly related with the slope dependent on the forcing regime. It is likely that the size distribution (and therefore $\overline{\sigma}$) is constant within each forcing regime and that the number of targets, N, increases with increase in flow. If $\overline{\sigma}$, and therefore bubble size distribution, had changed within a forcing regime then the bubble size distribution and scaling factor N would both have to scale linearly with flow rate, which is an unlikely scenario. The difference in slope between the two flow regimes is likely due to a change in $\overline{\sigma}$. Bubbles formed in the pressure driven regime experience an initial velocity when exiting the orifice that is likely to result in increased fractioning of bubble, and a decrease in droplet size when compared to droplets in the buoyancy driven regime.

SIGNAL TO NOISE RATIO AND DETECTION RANGE

The signal to noise ratio (SNR) for the maximum flow rate (2.65 l / min) and the minimum flow rate (0.115 l/min) as a function of distance from the echo sounder was calculated in order to determine the detection limit for the extrema of flow scenarios in this experiment. The SNR as a function is equal to

$$\text{SNR} = 10\log_{10}\left(\frac{TS\, e^{-4\alpha r}}{r^4}\left(\frac{r}{70}\right)\right) - NL, \quad (4)$$

where α is the absorption coefficient in units of nepers / meter and r is the range and NL is the noise level in dB. The $r/70$ term accounts for the change in beam width due to a change in range relative to the range at with the TS was measured. Assuming that the bubbles within the beam of the echosounder are uniformly distributed in a vertical column in the water column, the horizontally oriented beam of the echo sounder will decrease in size as the instrument approaches the bubbles. Therefore, the number of bubbles (N) will decrease proportional decrease or increase in the beam "footprint" for ranges other than the range at which TS was measured (70 m). The limit to detection was set to a SNR of 10 dB. In FM mode the limit for detection for the maximum flow rate (2.64 l/min) was 598 meters and 176 meters for the ES70 and ES333 respectively (Fig 5). For the minimum flow rate (0.115 l/min), broadband detection was limited to within 399 meters and 86 meters of the ES70 and ES333 respectively.

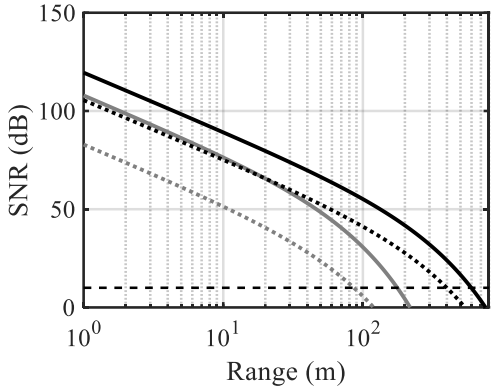

Fig. 5: The signal to noise ratio (SNR) as a function of range from the echo sounder for the maximum flow rate for the ES70 (solid black line) and ES333 (solid gray line) and the minimum flow rate for the ES70 (dashed black line) and ES333 (dashed gray line). The detection limit was set to 10 dB(horizontal dashed black line).

SNR of the seep was also determined for the ES70 in CW mode for the maximum leak rate of 2.65 liters / minute (Fig 6). The difference between the SNR in FM and CW mode was 25 dB, 5dB higher than the predicted increase in SNR for an matched filer FM pulse of 2 BT [12], [13], where B is the bandwidth and T is the pulse length.

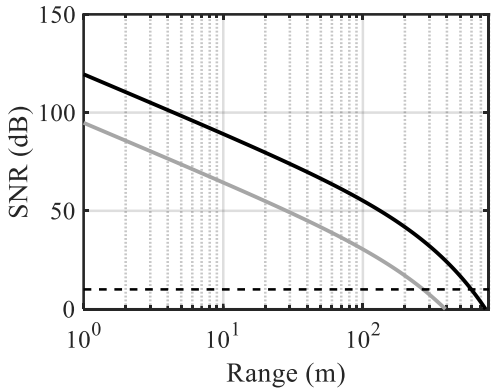

Fig. 6: The signal to noise ratio (SNR) as a function of range from the echo sounder for the maximum flow rate 2.6 liters / min for the ES70 in FM mode (solid black line) and the ES70 in CW mode (solid gray line) The detection limit was set to 10 dB (horizontal dashed black line).

CONCLUSIONS

The two broadband echo sounders were both capable of detecting the simulated seep for all flow rates. The TS of the seep in the ES333 was about 10 dB lower than that of the ES70. Bubble size appeared to be constant within each forcing regime; however, the size distribution appeared to change between forcing regimes, likely due to increased fractioning of bubbles due to the increased initial velocity in the pressure-forcing regime. The lower TS and increased attenuation of the higher frequency system resulted in significantly shorter detection ranges for the ES333 (176 m compared to 598 m for the ES70 at the highest flow rate). Operating the ES70 in FM (45

kHz to 95 kHz) mode resulted in an increased SNR of 25 dB relative to the same echo sounder in narrow band mode. The increased SNR was 5 dB higher than predicted.

While the ES70 had a higher SNR for the experiment conducted here, the appropriate frequency for monitoring GCS sites depends on the depth of the site. For sites below 600 m CO_2 will be in liquid form and higher frequencies are likely to be necessary.

The authors would like to acknowledge the ACT4storage Partners as well as the Norwegian Stat enterprise Gassnova for their support of this project.

REFERENCES

[1] IPCC, "Climate Change 2014: Synthesis Report. Contribution of Working Groups I, II and III to the Fifth Assessment Report of the Intergovernmental Panel on Climate Change," IPCC, Geneva, Switzerland, 2014.
[2] IEA Greenhouse Gas R&D Programme (IEA GHG), "Review of Offshore Monitoring for CCS Project," no. July, 2015.
[3] EU GeoCapacity, "Assessing European Capacity for Geological Storage of Carbon Dioxide," *D16 WP2 Storage Capacit.*, p. 170.
[4] IEA Greenhouse Gas R&D Programme (IEA GHG), "Assessment of sub sea ecosystem impacts," pp. 1–266, 2008.
[5] Directorate-General for Climate Action (European Commission), "Implementation of Directive 2009 / 31 / EC on the Geological Storage of Carbon Dioxide - Guidance Document 1: CO2 Storage Life Cycle Risk Management Framework," p. 54, 2009.
[6] S. Bourne, S. Crouch, and M. Smith, "A risk-based framework for measurement, monitoring and verification of the Quest CCS Project, Alberta, Canada," *Int. J. Greenh. Gas Control*, vol. 26, pp. 109–126, Jul. 2014.
[7] M. Dean and O. Tucker, "A risk-based framework for Measurement, Monitoring and Verification (MMV) of the Goldeneye storage complex for the Peterhead CCS project, UK," *Int. J. Greenh. Gas Control*, vol. 61, pp. 1–15, Jun. 2017.
[8] S. Hannis *et al.*, "Review of Offshore CO2 Storage Monitoring: Operational and Research Experiences of Meeting Regulatory and Technical Requirements," *Energy Procedia*, vol. 114, pp. 5967–5980, Jul. 2017.
[9] V. C. Anderson, "Sound Scattering from a Fluid Sphere," *J. Acoust. Soc. Am.*, vol. 22, no. 4, pp. 426–431, 1950.
[10] S. Loranger, C. Bassett, J. P. Cole, B. Boyle, and T. C. Weber, "Acoustically relevant properties of four crude oils at oceanographic temperatures and pressures," *J. Acoust. Soc. Am.*, vol. 144, no. 5, pp. 2926–2936, Nov. 2018.
[11] D. A. Demer *et al.*, "Calibration of acoustic instruments," *ICES Coop. Res. Rep.*, no. 326, 2015.
[12] D. Chu and T. K. Stanton, "Application of pulse compression techniques to broadband acoustic scattering by live individual zooplankton," *J. Acoust. Soc. Am.*, vol. 104, no. 1, pp. 39–55, Jun. 1998.
[13] G. L. Turin, "An Introduction to Matched Filters," *IRE Trans. Inf. Theory*, vol. IT-6, pp. 311–329, 1960.